

# High-contrast grating MEMS optical phase-shifters for two-dimensional free-space beam steering

Mischa Megens<sup>a</sup>, Byung-Wook Yoo<sup>b</sup>, Trevor Chan<sup>a</sup>, Weijian Yang<sup>b</sup>, Tianbo Sun<sup>b</sup>,  
Connie J. Chang-Hasnain<sup>b</sup>, Ming C. Wu<sup>b</sup>, and David A. Horsley<sup>a,\*</sup>

<sup>a</sup>Department of Mechanical and Aerospace Engineering, University of California at Davis, Davis, California 95616, United States; <sup>b</sup>Department of Electrical Engineering and Computer Sciences, University of California, Berkeley, CA 94720, United States

## ABSTRACT

We report an optical phased array (OPA) for two-dimensional free-space beam steering. The array is composed of tunable MEMS all-pass filters (APFs) based on polysilicon high contrast grating (HCG) mirrors. The cavity length of each APF is voltage controlled via an electrostatically-actuated HCG top mirror and a fixed DBR bottom mirror. The HCG mirrors are composed of only a single layer of polysilicon, achieving >99% reflectivity through the use of a subwavelength grating patterned into the polysilicon surface. Conventional metal-coated MEMS mirrors must be thick (1-50  $\mu\text{m}$ ) to prevent warpage arising from thermal and residual stress. The single material construction used here results in a high degree of flatness even in a thin 350 nm HCG mirror. Relative to beamsteering systems based on a single rotating MEMS mirror, which are typically limited to bandwidths below 50 kHz, the MEMS OPA described here has the advantage of greatly reduced mass and therefore achieves a bandwidth over 500 kHz. The APF structure affords large ( $\sim 2\pi$ ) phase shift at a small displacement ( $< 50$  nm), an order-of-magnitude smaller than the displacement required in a single-mirror phase-shifter design. Precise control of each all-pass-filter is achieved through an interferometric phase measurement system, and beam steering is demonstrated using binary phase patterns.

**Keywords:** optical phased arrays, beam steering, micro electro mechanical systems, high contrast gratings, Gires-Tournois etalon, all-pass filters.

## 1. INTRODUCTION

Optical phased arrays (OPAs)<sup>1,2</sup> are versatile beam steering devices suitable for a variety of applications including LIDAR, free-space optical communication, 3D holographic displays, and high-resolution 3D imaging.<sup>3,4</sup> An OPA consists of a two-dimensional (2D) array of phase shifters which impose a desired phase profile on an incoming beam of light. The constructive interference of the outgoing light waves forms the desired beam. An OPA is usually much faster than a single steering mirror, as individual phase shifters are much smaller and more nimble than a large scanning mirror.

The dominant OPA technology is based on liquid crystal phase shifters, which have been studied extensively since their initial demonstration using liquid crystal television panels.<sup>5,6</sup> However, liquid crystals have limited operating speed because it takes tens of milliseconds for an electric field to reorient the molecules of the liquid crystal. More recently, micro-electromechanical systems (MEMS) have been used to produce OPAs.<sup>7,8</sup> A typical MEMS-based phase shifter is realized by a “piston” mirror which is displaced to provide the desired phase shift. To increase the speed of such MEMS-based beam steering, we recently introduced phased arrays based on high contrast gratings (HCG’s), rather than mirrors.<sup>9-11</sup> Unlike earlier multi-layer MEMS mirrors, these grating mirrors are made of a single dielectric layer, achieving high reflectivity ( $\sim 99.9\%$ ) over a broad optical bandwidth.<sup>9,12</sup> The HCG’s single-material construction results in greater manufacturability since residual stress is easily controlled when depositing the single polysilicon layer and the process eliminates the need for non-CMOS compatible metals such as gold. The HCG-OPA has the potential to operate at high optical power without warping due to mismatch in coefficient of thermal expansion and without the thermal damage that plagues mirrors composed of low melting-point metals (e.g. Au and Al). The thin, open structure of the grating mirrors greatly reduces its mass, and this increases the operating bandwidth of the OPA.

\* dahorsley@ucdavis.edu; phone: 1-530-341-3236, fax: 1-530-752-4158

Our HCG OPA's are electrostatically actuated by applying a voltage between the movable mirror and the substrate underneath. Achieving a full  $2\pi$  phase shift requires a mirror displacement of half a wavelength. To avoid pull-in, the displacement should remain smaller than about one-third of the gap between the electrodes. The gap needs to be sufficiently large to accommodate the desired stroke. This either leads to a high actuation voltage, or it requires softening the springs, which impacts the operating bandwidth.

Here we demonstrate a way to reduce the operating voltage, or further increase the beam steering speed, by employing not just a single mirror element for each phase shifter but rather a highly reflective mirror pair that forms a Gires-Tournois etalon. The bottom mirror in such an etalon is designed to have a reflectivity much closer to 100% than the top mirror, so the etalon acts as an all-pass filter: nearly all the incident light is always reflected, regardless of the mirror separation. However, the phase abruptly changes by  $2\pi$  radians when the etalon moves through a resonance, i.e., when the optical path length of a round trip between the two mirrors changes from slightly shorter to slightly longer than an integer number of wavelengths. The gap between our mirror pair is perched close to such a resonance, so that a slight electrostatic attraction of the top mirror to the bottom mirror will result in a large phase shift. The steepness of the phase shift relates to the reflectivity of the top mirror and can be designed to match the stroke of the electrostatic actuation. Using this concept, we designed a phase shifter with a bandwidth over 500 kHz, large phase shifts, yet a low actuation voltage. We demonstrate beam steering with an  $8\times 8$  array of such all-pass-filter mirrors.

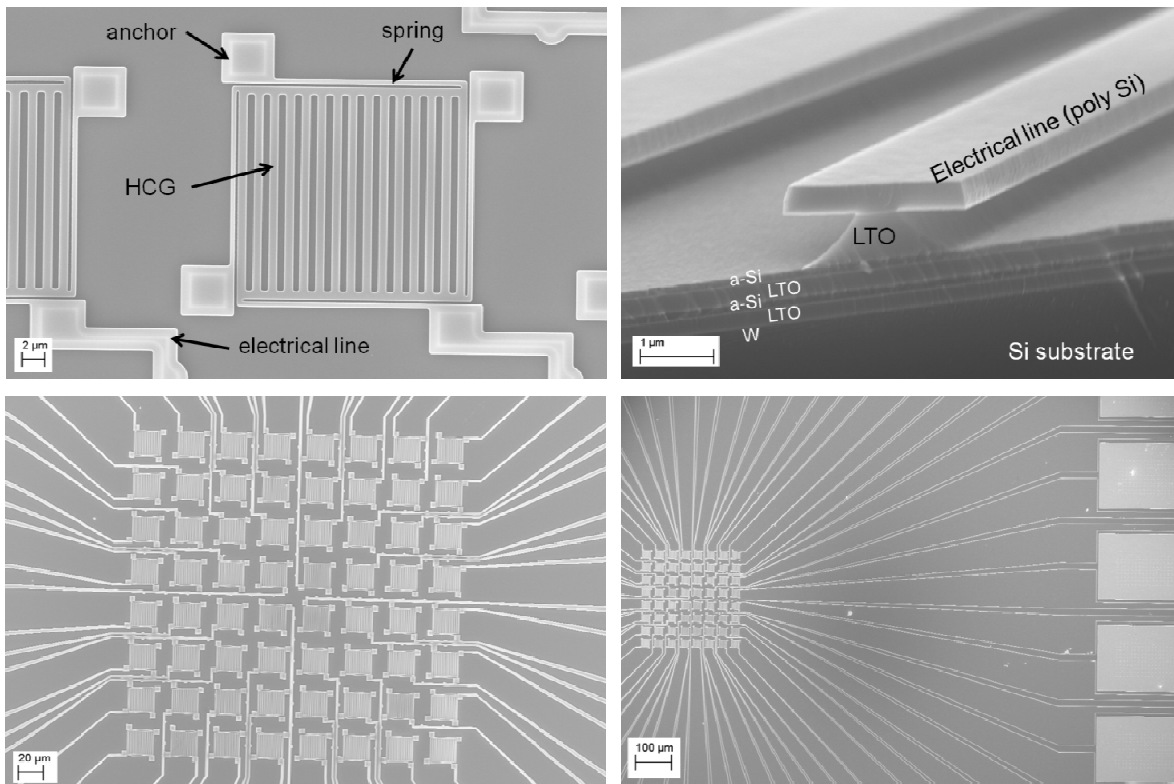


Figure 1. Scanning electron micrographs of a High Contrast Grating (HCG) mirror array, on top of a DBR mirror in the substrate. Together the two mirrors form a Gires-Tournois etalon. The HCG mirror is suspended from four flexure springs, allowing it to move out of plane. It can be electrostatically actuated by applying a voltage between the polysilicon grating layer and the tungsten ground plane in the substrate. An  $8\times 8$  array of these phase shifters forms a phased array for beam steering.

## 2. PHASE SHIFTER DESIGN

Figure 1 shows the construction of a single phase shifter element. It consists of a high contrast grating mirror of submicron polysilicon bars in a firm square frame. The frame is suspended from four thin flexure springs that allow the grating to move towards the substrate. The flexure springs are attached to the substrate using square anchor pads supported by a silicon oxide column. The substrate incorporates a distributed Bragg reflector (DBR) mirror that consists of a tungsten film beneath two pairs of amorphous silicon/silicon oxide. The mirror can be electrostatically actuated by applying a voltage between the tungsten and the highly doped polysilicon grating, via the anchor pads. The pads are electrically insulated from the substrate by silicon oxide. The same oxide serves as the sacrificial layer for releasing the polysilicon; it also supports the electrical wiring that connects the individual mirrors to their voltage source. Figure 1(b) provides a cross section view, showing the polysilicon wiring, supported by the low temperature oxide, and the distributed Bragg reflector mirror underneath. An 8 by 8 array of such phase shifters is shown in Figure 1(c). Each HCG covers an area of  $20 \times 20 \mu\text{m}^2$ . The mirror pitch is  $35 \mu\text{m}$ , i.e., the fill factor is  $\sim 33\%$ . The phase shifters are individually addressable, and together form an optical phased array that enables beam steering.

The bottom DBR mirror of the phase shifter is designed to have a higher reflectivity than the HCG mirror above, so most of the light incident on the mirror pair will be reflected back, but with a phase shift that depends on the mirror separation. Suitable phase shifts for the phased array can be obtained by tuning through the etalon resonance, by applying the proper voltage to electrostatically attract the grating mirror to the DBR substrate. To quantitatively understand the phase of such a mirror pair, it is helpful to consider the simpler case of a Fabry-Pérot interferometer formed by a thin transparent plate on a highly reflective substrate, as shown in Figure 2(a).

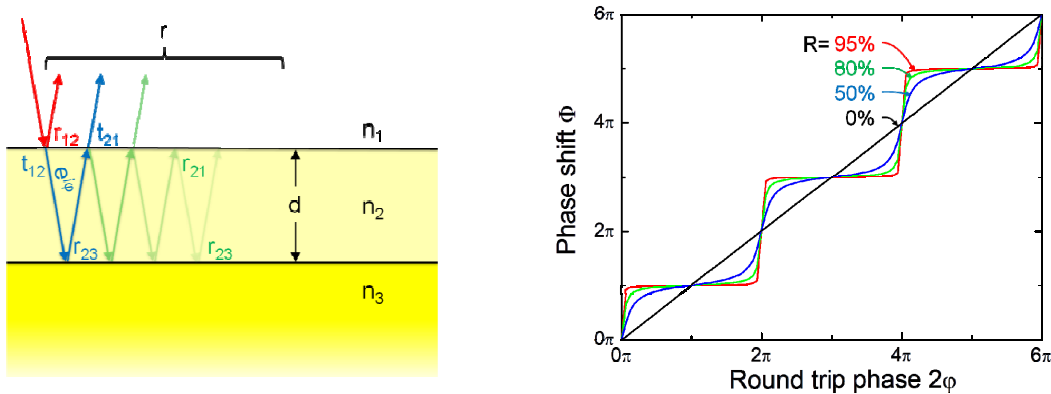


Figure 2. A Gires-Tournois etalon, consisting of a transparent layer (2) on a highly reflective substrate (3). Light incident on the etalon can experience multiple round trips between the interfaces (shown here at a slight angle for clarity). The graph shows the optical phase of the combined reflections vs. round trip phase (i.e., twice the optical thickness of the middle layer), for various reflectivities  $R$  of the top interface of 0, 50, 80, and 95%. For 0% the top mirror is absent, and the phase shift measured from the top interface equals the round trip phase to the bottom mirror; for higher  $R$  the change in phase increasingly becomes concentrated near thicknesses that are half-integer multiples of the wavelength.

The multiple reflections between the two interfaces add up coherently, and their combined amplitude reflection coefficient of the etalon is

$$r = r_{12} + \frac{t_{12}t_{21}r_{23}e^{2i\varphi}}{1 - r_{21}r_{23}e^{2i\varphi}}, \quad (1)$$

where we have used that  $\sum_{m=0}^{\infty} z^m = 1/(1-z)$  to sum the contributions from repeated reflections between the two mirror surfaces. The reflection and transmission coefficients are labeled as indicated in Figure 2, and the round trip phase  $2\varphi = 4\pi d/\lambda$ , with  $d$  the thickness of the transparent layer, and  $\lambda$  the wavelength of the light. For normal incidence, the Fresnel coefficients are  $r_{12} = (n_1 - n_2)/(n_1 + n_2)$  and  $t_{12} = 2n_1/(n_1 + n_2)$ , so  $r_{12} = -r_{21}$ . These Fresnel coefficients are related to the reflection  $R$  and transmission  $T$  of the top interface via  $R = |r_{12}|^2 = |r_{21}|^2$  and

$T = t_{12}t_{21}$ . Any light not reflected must be transmitted, so  $T = 1 - R$ ; this further simplifies equation (1). If we set  $n_3 = 0$  to make the bottom interface highly reflective, then we arrive at the familiar Gires-Tournois result:

$$r = -\frac{\sqrt{R} - e^{2i\varphi}}{1 - \sqrt{R}e^{2i\varphi}}. \quad (2)$$

The phase shift  $\Phi$  follows from  $r = |r|e^{i\Phi}$ :

$$\tan \frac{\Phi}{2} = \frac{1 + \sqrt{R}}{1 - \sqrt{R}} \tan \varphi \quad (3)$$

(Alternatively, the bottom interface can also be made highly reflective by setting  $n_3 = \infty$ , more akin to a metallic interface. This results in a sign change for  $r_{23}$ , and hence an additional  $\pi$  phase shift.) Graphs of the phase shift are shown in Figure 2(b), for various reflectivities  $R$  of the top interface. The phase shift here is measured from the top interface. If its reflectivity is 0%, then the top interface might as well not be there, so the phase shift equals the round trip phase to the bottom mirror, and the graph is a straight line. For higher  $R$ , the phase shift becomes almost constant, except for increasingly steep steps of  $2\pi$  near the resonances, where the optical path length of a mirror round trip equals an integer number of wavelengths. It is near such a resonance that we want to poise our etalon, so a small change in mirror separation leads to a large change in phase.

The calculation of the etalon reflectivity for an HCG-DBR mirror pair closely follows the development above. Since the mirrors are now no longer infinitely thin, we have to be more specific about the phase. We define the reflection and transmission phase with respect to the outer surfaces of the mirrors, as shown in Figure 3. The Figure also shows the dimensions of the HCG and the DBR layers. The dimensions are designed so that the reflectivity of the HCG is lower than that of the DBR. The HCG dimensions are optimized to provide a large window of fabrication tolerance.<sup>10</sup>

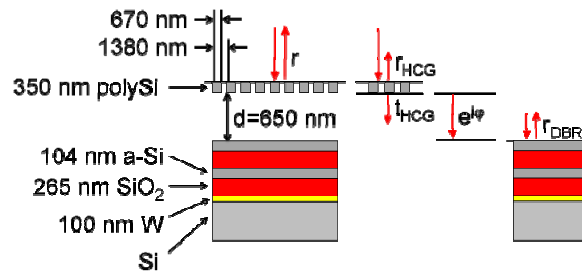


Figure 3. A Gires-Tournois etalon using a high contrast grating (HCG) mirror on top, and a distributed Bragg reflector (DBR) mirror below, with dimensions of the mirror components indicated. The reflection of the mirror pair can be understood in terms of the reflection and transmission of its components, as shown.

Since the polysilicon HCG mirror is not absorbing, it is still true that  $T = 1 - R$ . With our definition of the phase with respect to the outer planes of the high contrast grating, it turns out that  $\arg(t) = \arg(r) + \pi/2$ , and we find that

$$r = e^{i\varphi_{\text{HCG}}} \frac{|r_{\text{HCG}}| - |r_{\text{DBR}}|e^{2i\varphi}}{1 - |r_{\text{HCG}}||r_{\text{DBR}}|e^{2i\varphi}}, \quad (4)$$

where the round trip phase  $2\varphi$  now incorporates the phase shifts of the HCG and the DBR reflections:

$$2\varphi = \varphi_{\text{HCG}} + \varphi_{\text{DBR}} + 2\pi \frac{2(d - \Delta)}{\lambda}, \quad (5)$$

where  $\Delta$  is the electrostatic displacement of the HCG. The resulting phase shift of the etalon is

$$\Phi = \varphi_{\text{HCG}} + \arctan \left( \frac{1 + \sqrt{R_{\text{HCG}} \cdot R_{\text{DBR}}}}{1 - \sqrt{R_{\text{HCG}} \cdot R_{\text{DBR}}}} \tan \varphi \right) + \arctan \left( \frac{1 + \sqrt{R_{\text{HCG}}/R_{\text{DBR}}}}{1 - \sqrt{R_{\text{HCG}}/R_{\text{DBR}}}} \tan \varphi \right) + \pi. \quad (6)$$

Since  $R_{\text{DBR}}$  is close to 1, the two arctangent terms are almost equal, and furthermore the  $R_{\text{DBR}}$  and  $1/R_{\text{DBR}}$  in these terms tend to cancel, hence the phase shift of our device is closely approximated by

$$\Phi = \varphi_{\text{HCG}} + 2 \arctan \left( \frac{1 + \sqrt{R_{\text{HCG}}}}{1 - \sqrt{R_{\text{HCG}}}} \tan \varphi \right) + \pi + 2\pi \frac{2\Delta}{\lambda}. \quad (7)$$

The last term takes into account that in our device, the substrate is stationary and the front surface is moving, leading to an extra phase delay if the phase shifter is actuated. In contrast, the phase due to the resonance (the arctangent) changes in the opposite direction. Hence the achievable phase shift is slightly smaller than  $2\pi$ . Fortunately this is of little consequence in practice, since the phase change due to resonance is much larger than that due to displacement of the front surface.

### 3. RESULTS AND DISCUSSION

Figure 3 shows the phase shift versus wavelength of one of the all pass filter mirrors in our array. The phase was measured using phase shifting interferometry as outlined in ref. 11, using a tunable laser source. The phase is referenced to the phase of a reflection from the area in between the mirrors nearby. The phase shows a large change of close to  $2\pi$  going across the resonance of the all-pass filter. Applying a modest voltage attracts the HGC mirror towards the DBR and shifts the resonance toward shorter wavelengths, as expected.

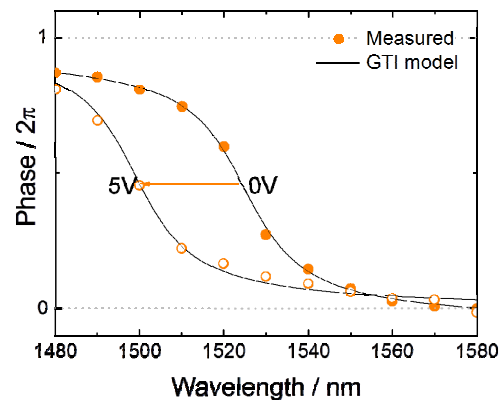


Figure 4. Measured phase shift vs. wavelength of the all-pass filter mirror of Figure 3. The curves are a fit to Eq. 7, phase shift for a Gires-Tournois etalon. Applying a voltage actuates the mirror and shifts the resonance, as expected.

Figure 5 provides a further confirmation that the phase shifter is working as designed. This Figure shows the phase shift vs. voltage squared for several wavelengths. Plotting vs. squared voltage puts these curves on the same footing, since the mirror displacement is expected to be approximately proportional to voltage squared, for electrostatic actuation. The HCG and DBR mirrors are sufficiently broadband reflectors that the reflectivity is similar for the various wavelengths, but the round trip phase changes, so the curves shift accordingly.

Positioning the mirrors close to resonance to achieve low voltage operation requires careful design of the HCG and DBR, since the round trip phase due to the mirrors is about equally important as that due to the mirror separation. Changing the operating wavelength provides some latitude, but not very much, as will be clear from Figure 5. In particular, if the mirror gap is too narrow, then no applied voltage can bring the etalon back into resonance. For the phase shifters demonstrated here, we selected an operating wavelength of 1500 nm to comfortably perform beam steering.

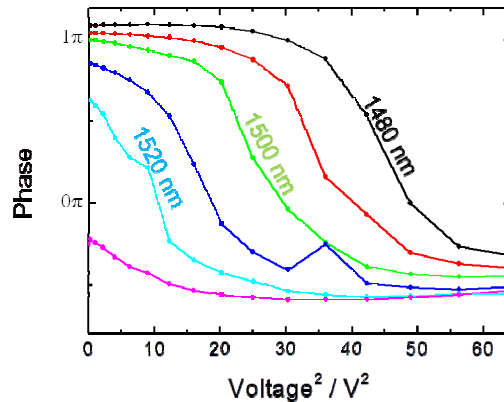


Figure 5. Measured phase shift vs. voltage squared, for various wavelengths from 1480 nm to 1530 nm, in 10 nm increments.

To put the advantage of an all-pass filter mirror in perspective, we compare its phase shift with that achieved by reflecting from the surface of a single actuated HCG mirror, in Figure 6. The HCG-only mirror is comparable in design to the all-pass filter HCG.<sup>12</sup> In particular, it has similar resonant frequency. For the conventional HCG mirror, the phase increases with voltage, as the mirror gradually is pulled in. Since the displacement varies quadratically with voltage, the phase varies quadratically too. In contrast, the phase of the all-pass filter mirror decreases as the etalon tunes through the resonance. From the Figure it is apparent that the all-pass filter provides a larger phase shift for a considerably reduced actuation voltage.

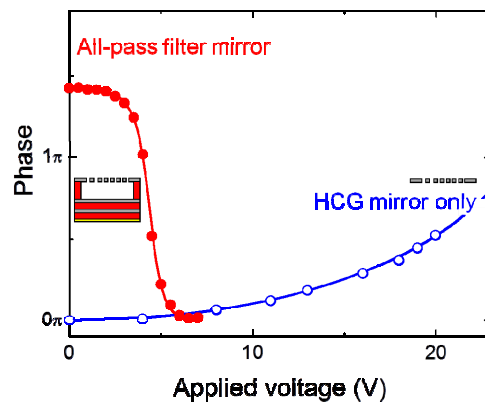


Figure 6. Comparison of the phase shift of our HCG-DBR all-pass filter phase shifter (red, filled symbols) with the phase shift of a single HCG phase shifter (blue, open symbols), with similar resonant frequency. The all-pass filter achieves a larger phase shift for a much reduced actuation voltage.

Beam steering experiments were conducted with the  $8 \times 8$  array of mirrors using a binary pattern of phase shifts, i.e., with the phase of the mirrors set to either 0 or  $\pi$  radians. Far field images for a selection of patterns are shown in Figure 7. The central spot in these images is the 0<sup>th</sup> order beam due to the modest 33% fill factor of the present array. The binary patterns shown deflect the beam symmetrically to the four corners of the field (for the checkerboard pattern), or up and down (for a pattern of horizontal lines), to left and right (for vertical lines), or diagonally (for a diagonal line

pattern). Smaller deflection angles can be obtained by applying a more coarsely structured pattern, as illustrated with the checkerboard pattern. In fact, any beam position inside the dashed square can be reached by applying a suitable pattern. A video of the beam raster scanning over the square is available online.

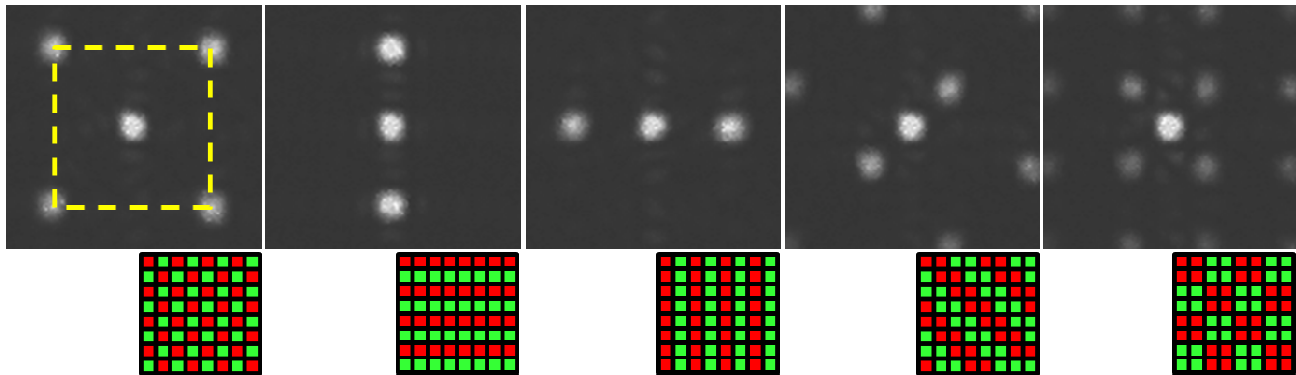
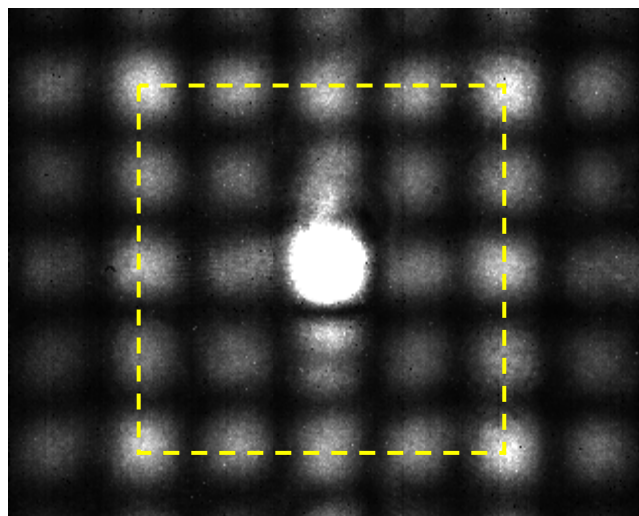


Figure 7. A selection of beam patterns. The dashed rectangle in the first panel outlines the maximum steering range. The pattern below each panel shows the arrangement of mirrors switched on or off ( $\pi$  or zero phase shift).



Video 8. Beam steering. Images for multiple beam positions are superimposed here. A video of the beam making a raster scan is available at: <http://dx.doi.org/10.1117/12.2045341.1>

#### 4. CONCLUSIONS

A novel micro-electromechanical systems optical phase shifter based on an all-pass filter has been successfully developed for fast beam steering. The  $8 \times 8$  array of phase shifters consist of lightweight high contrast grating mirrors suspended above a distributed Bragg reflector mirror substrate using flexure springs. The mirrors are electrostatically actuated by applying a voltage between a grating mirror and the substrate. The mirror separation is designed such that the mirror pair is poised close to resonance, where the round trip optical path length is slightly longer than an integral number of wavelengths. A small mirror displacement then suffices to pull the mirrors through resonance, leading to a large voltage-controlled phase shift. In this way we achieve a wide operating bandwidth of over 500 kHz, for a low actuation voltage. We demonstrate beam steering with an  $8 \times 8$  array of these all-pass-filter mirrors.

## ACKNOWLEDGEMENTS

This work was supported by the DARPA SWEEPER program (Grant No. HR0011-10-2-0002). Devices were fabricated at the Marvell Nanofabrication Laboratory at UC Berkeley.

## REFERENCES

- [1] Sun, J., Timurdogan, E., Yaacobi, A., Hosseini, E.S., and Watts, M.R., "Large-scale nanophotonic phased array," *Nature* 493(7431), 195–199 (2013).
- [2] McManamon, P.F., Bos, P.J., Escuti, M.J., Heikenfeld, J., Serati, S., Xie, H., and Watson, E.A., "A Review of Phased Array Steering for Narrow-Band Electrooptical Systems," *Proceedings of the IEEE* 97, 1078–1096 (2009).
- [3] Doyle, J.K., Heck, M.J.R., Bovington, J.T., Peters, J.D., Coldren, L.A., and Bowers, J.E., "Two-dimensional free-space beam steering with an optical phased array on silicon-on-insulator," *Optics Express* 19, 21595–21604 (2011).
- [4] McManamon, P.F., Dorschner, T.A., Corkum, D.L., Friedman, L.J., Hobbs, D.S., Holz, M., Liberman, S., Nguyen, H.Q., Resler, D.P., et al., "Optical phased array technology," *Proceedings of the IEEE* 84, 268–298 (1996).
- [5] Engstrom, D., O'Callaghan, M.J., Walker, C., and Handschy, M.A., "Fast beam steering with a ferroelectric-liquid-crystal optical phased array," *Applied Optics* 48, 1721–1726 (2009).
- [6] Jau, H.C., Lin, T.H., Fung, R.X., Huang, S.Y., Liu, J.H., and Fuh, A.Y.G., "Optically-tunable beam steering grating based n azobenzene doped cholesteric liquid crystal," *Optics Express* 18, 17498–17503 (2010).
- [7] Bifano, T.G., Perreault, J., Mali, R.K., and Horenstein, M.N., "Microelectromechanical deformable mirrors," *IEEE Journal of Selected Topics in Quantum Electronics* 5, 83–89 (1999).
- [8] Krishnamoorthy, U., Li, K., Yu, K., Lee, D., Heritage, J.P., and Solgaard, O., "Dual-mode micromirrors for optical phased array applications," *Sensors and Actuators A-Physical* 97-8, 21–26 (2002).
- [9] Yoo, B.W., Megens, M., Chan, T., Sun, T., Yang, W., Chang-Hasnain, C.J., Horsley, D.A., and Wu, M.C., "Optical phased array using high contrast gratings for two dimensional beamforming and beamsteering," *Optics Express* 21, 12238–12248 (2013).
- [10] Chan, T.K., Megens, M., Yoo, B.W., Wyrwas, J., Chang-Hasnain, C.J., Wu, M.C., and Horsley, D.A., "Optical beamsteering using an  $8 \times 8$  MEMS phased array with closed-loop interferometric phase control," *Optics Express* 21, 2807–2815 (2013).
- [11] Yoo, B.W., Megens, M., Chan, T.K., Sun, T., Yang, W., Horsley, D.A., Chang-Hasnain, C.J., and Wu, M.C., "32x32 Optical phased array with ultra-lightweight high-contrast-grating mirrors," presented at Proc. 17th Intl. Conf. on Solid-State Sensors Actuators and Microsystems, 16 June 2013, 2505–2508.
- [12] Huang, M.C.Y., Zhou, Y., and Chang-Hasnain, C.J., "A surface-emitting laser incorporating a high-index-contrast subwavelength grating," *Nature Photonics* 1, 119–122 (2007).